Seasonal Variations in the Siliciclastic Fluxes to the Western Philippine Sea and Their Impacts on Seawater Nd Values Inferred From 1 Year of In Situ Observations Above Benham Rise

Zhaokai Xu, Tiegang Li, Christophe Colin, Peter D. Clift, Rongtao Sun, Zhaojie Yu, Shiming Wan, Dhongil Lim

AGU100 ADVANCING EARTH AND SPACE SCIENCE

JGR

Journal of Geophysical Research: Oceans

RESEARCH ARTICLE
10.1029/2018JC014274

Key Points:
- The eolian dust sources to the western Philippine Sea are determined and quantified
- The impacts of the East Asian monsoon on the siliciclastic fluxes to the Benham Rise are characterized
- Rapid changes in planktonic foraminiferal ε_{Nd} values occur during settling in the ocean

Correspondence to:
T. Li and D. Lim,
tgli@fio.org.cn;
oceanlim@kiost.ac.kr

Citation:
Xu, Z., Li, T., Colin, C., Clift, P. D., Sun, R., Yu, Z., et al. (2018). Seasonal variations in the siliciclastic fluxes to the western Philippine Sea and their impacts on seawater ε_{Nd} values inferred from 1 year of in situ observations above Benham Rise. *Journal of Geophysical Research: Oceans*, *123*, 6688–6702. https://doi.org/10.1029/2018JC014274

Received 7 JUL 2018
Accepted 21 AUG 2018
Accepted article online 29 AUG 2018
Published online 19 SEP 2018

Seasonal Variations in the Siliciclastic Fluxes to the Western Philippine Sea and Their Impacts on Seawater ε_{Nd} Values Inferred From 1 Year of In Situ Observations Above Benham Rise

Zhaokai Xu[1,2], Tiegang Li[2,3,4], Christophe Colin[5], Peter D. Clift[6,7], Rongtao Sun[8], Zhaojie Yu[1,5], Shiming Wan[1,2], and Dhongil Lim[9]

[1]CAS Key Laboratory of Marine Geology and Environment, Institute of Oceanology, Chinese Academy of Sciences, Qingdao, China, [2]Laboratory for Marine Geology, Qingdao National Laboratory for Marine Science and Technology, Qingdao, China, [3]Key Laboratory of Marine Sedimentology and Environmental Geology, First Institute of Oceanography, SOA, Qingdao, China, [4]University of Chinese Academy of Sciences, Beijing, China, [5]Laboratoire GEOsciences Paris-Sud (GEOPS), UMR 8148, CNRS-Université de Paris-Sud, Université de Paris-Saclay, Orsay Cedex, France, [6]Department of Geology and Geophysics, Louisiana State University, Baton Rouge, LA, USA, [7]School of Geography Science, Nanjing Normal University, Nanjing, China, [8]School of Resources and Environment Engineering, Shandong University of Technology, Zibo, China, [9]South Sea Research Institute, Korea Institute of Ocean Science & Technology, Geoje, South Korea

Abstract The Sr and Nd isotopic compositions of siliciclastic sediments and the Nd isotopic compositions of planktonic foraminifera are investigated in sediment trap samples collected in 2015 at water depths of 500 and 2,800 m to (1) track the seasonal changes in the sources and transport patterns of siliciclastic sediments to Benham Rise, (2) constrain the Nd isotopic compositions of the planktonic foraminifera throughout the water column, and (3) assess the influences of lithogenic inputs on the Nd isotopic compositions of the water masses. We demonstrate that volcanic matter and eolian dust are derived primarily from Luzon Island and the Ordos Desert, respectively. In addition, we show that reduced precipitation over Luzon Island and the weakened East Asian winter monsoon intensity result in mass fluxes from Luzon Island and the eastern Asian deserts to the sea, respectively, that are weaker in the winter than in the spring. Furthermore, the ε_{Nd} values of the foraminifera collected at a water depth of 500 m change slightly in 2015, suggesting negligible impacts of lithogenic Nd inputs characterized by significant seasonal flux variations. In contrast, the ε_{Nd} values of the planktonic foraminifera collected at a water depth of 2,800 m are systematically more radiogenic and appear to display seasonal variability. Such results suggest the rapid modification of ε_{Nd} values during the settling of planktonic foraminifera by the precipitation of Mn coatings derived from water masses at deposition depths, with greater contributions of colder water masses originating from the volcanic Luzon Island margin during the winter.

Plain Language Summary Based on the first report of Sr-Nd isotopic compositions of siliciclastic sediments and Nd isotopic compositions of planktonic foraminifera in sediment trap samples collected from the western Philippine Sea in 2015 at water depths of 500 and 2,800 m together with the relevant current information, we try to recover the potential linkages between the East Asian winter monsoon strength, the East Asian summer monsoon (precipitation) intensity, and the siliciclastic sediment source-to-sink processes as well as the influences of lithogenic inputs on the Nd isotopic compositions of the water masses at the northern margin of the western Pacific Warm Pool in different seasons of 2015. On the one hand, we quantitatively estimate the eolian dust sources to the study area. On the other hand, we find the rapid changes in planktonic foraminiferal ε_{Nd} values during settling in the western Philippine Sea. Such results are critical for effectively interpreting the siliciclastic sediment source-to-sink processes and marine circulation as well as the behind controlling mechanisms at low latitudes during the geological past.

1. Introduction

Eolian dust plays a crucial role in the marine and terrestrial geochemical cycles and impacts global climate change by scattering and absorbing solar radiation, changing cloud properties, affecting biogeochemical cycles, and providing key surfaces for atmospheric reactions in the Earth-atmosphere-ocean system (Zhao et al., 2014). Each year, approximately 2000 million tons of eolian dust is emitted and deposited; 75% of

this dust is deposited on land, and 25% is deposited in the ocean (Shao et al., 2011). Eolian dust is mainly transported to the Pacific Ocean by the westerlies and the East Asian winter monsoon (EAWM) from mainland Asia, which constitutes the second most important dust source region on Earth (Zhao et al., 2014). It is generally accepted that eolian dust transported to the northern Pacific Ocean is derived primarily from the central Asian deserts (CADs; Zhao et al., 2014). In contrast, dust from the eastern Asian deserts (EADs) is predominantly transported southeastward to the northwestern Pacific Ocean, including the Philippine Sea (Jiang et al., 2013; Xu et al., 2015; Zhao et al., 2014). In particular, several studies have demonstrated that the EADs may be more important in controlling the supply of eolian dust than the CADs in these areas (Bird et al., 2015; Wang et al., 2015). Seo et al. (2014) recently suggested that the long-range transport of CAD dust by the westerlies is an important element of the dust budget in the northwestern Pacific Ocean. Therefore, the EADs and the CADs have been accepted as the most important Asian dust sources for the Philippine Sea (Seo et al., 2014; Xu et al., 2015; Zhao et al., 2014), although the relative importance of these sources is controversial (Seo et al., 2014; Xu et al., 2015).

The East Asian monsoon influences both the inputs of Asian dust and the precipitation over southeastern Asia; generally high precipitation but low air temperatures are observed over eastern Luzon Island in the winter (from October to December) and spring (from January to March), while generally low precipitation but high air temperatures are recorded over eastern Luzon Island in the summer (from April to June) and autumn (from July to September; http://www.worldweatheronline.com). The sediment inputs to the Benham Rise result from the mixing of two end-members, namely, eolian dust from the Asian deserts and fluvial particulates from Luzon Island; the relative contributions from these sources change over time due to variations in rainfall (Yu et al., 2016). Mineralogical records of the Benham Rise have already been used successfully to track past changes in eolian and riverine inputs and to extract records of monsoon rainfall over Luzon Island during the Quaternary (Yu et al., 2016). However, the influences of monsoon on rainfall and sediment transport to the Benham Rise remain speculative at present and need to be further explored. Therefore, only a detailed study of the processes by which siliciclastic inputs were delivered to the western Philippine Sea in 2015 permits us to test the hypothesis of a potential link between precipitation over volcanic islands and siliciclastic inputs to the deep sea, as suggested by previous research on Quaternary sediments from the Benham Rise (Jiang et al., 2016; Yu et al., 2016).

Because the residence time of Nd in the ocean (360–700 years; Siddall et al., 2008; Tachikawa et al., 2003) is short compared with the global turnover time of the ocean (~1,000 years), the distribution of the isotopic compositions of dissolved Nd in the ocean is heterogeneous (Tachikawa et al., 2017). This dissolved Nd is derived from (1) lithogenic inputs by rivers and wind transport from sedimentary sources of various ages (Jeandel & Oelkers, 2015), (2) boundary exchange processes that occur at continental margins (Grenier et al., 2013), and (3) reversible scavenging of lithogenic particulates in the water column (Siddall et al., 2008). ε_{Nd} has been widely used as a tracer for both modern (Tachikawa et al., 2017) and past oceanic circulation as well as continental weathering over different time scales (Colin et al., 2010). Recent studies have also shown that the Nd isotopic compositions of modern seawater may be strongly impacted by seasonal changes in the lithogenic inputs of eolian dust, deep-sea current loads, and riverine particulates (Laukert et al., 2017; Molina-Kescher et al., 2014; Yu et al., 2017). Due to boundary exchange processes with volcanic sediments from the western margins of the Pacific Ocean, the Nd isotopic signatures of water masses from the Philippine Sea are relatively radiogenic; the corresponding values are slightly elevated in deeper water masses (between -4.4 ± 0.3 and -3.0 ± 0.3; Wu et al., 2015) relative to those of southeastern samples in the western Pacific that are far away from these volcanic margins (Behrens et al., 2018). The ε_{Nd} values of core-top siliciclastic sediments recovered from the western Philippine Sea (Benham Rise) are between +0.7 and +2.2; these values represent the dominant contributions from radiogenic volcanic particulates derived from Luzon Island, which is characterized by values between +5.8 and +7.1 (Defant et al., 1990; Goldstein & Jacobsen, 1988; Liu et al., 2016) and nonradiogenic Asian dust, the values of which fall between −11.3 and −10.6 (Chen et al., 2007; Xu et al., 2015). The values of these sources contrast with those of seawater (which range from -4.4 ± 0.3 to -3.0 ± 0.3; Wu et al., 2015). This strong difference in the ε_{Nd} values between detrital sediments and seawater means that the Philippine Sea is a key area where the seasonal effects of lithogenic inputs, including eolian dust from Asian deserts and volcanic sediments from Luzon Island, on the Nd isotopic compositions of the seawater can be assessed, similar to the Panama Basin in the eastern equatorial Pacific (Grasse et al., 2017).

In addition, the ε_{Nd} values measured from fossil planktonic foraminifera may be unrelated to the ambient seawater at calcification depths; instead, they likely reflect the bottom and/or pore water ε_{Nd} values because of the precipitation of authigenic Mn coatings on their carbonate shells at deposition depths (Roberts et al., 2012; Tachikawa et al., 2014; Wu et al., 2017). Pomiès et al. (2002) also demonstrated that authigenic Mn coatings on planktonic foraminifera can develop within the water column; these coatings are derived ultimately from the water masses at deposition depths of these foraminifera. This process may significantly modify the Nd isotopic compositions of the foraminifera in the water column and thus effectively reflect the ε_{Nd} values of source water masses at particular water depths, which are hard to constrain, because measurements of the Nd isotopic compositions of the planktonic foraminifera collected in the water column were unavailable (Pomiès et al., 2002).

In this study, for the first time, we present 1 year of in situ mooring observations to quantify the sediments transported to the western Philippine Sea (above the Benham Rise) and characterize their variability. Moreover, we constrain the impacts of seasonal terrigenous inputs on the Nd isotopic compositions of the water masses reconstructed using the ε_{Nd} values of planktonic foraminifera. The siliciclastic sediment fractions and planktonic foraminifera were collected in 2015 at water depths of 500 and 2,800 m using a mooring system equipped with sediment traps, recording current meters, and conductivity-temperature-depth sensors. The characterizations of $^{87}Sr/^{86}Sr$ ratios and ε_{Nd} values have previously been shown to be extremely useful in establishing and quantifying Asian dust sources to the Pacific Ocean (Chen et al., 2007; Jiang et al., 2013; Mahoney, 2005; Seo et al., 2014; Serno et al., 2014; Xu et al., 2015). Therefore, our results permit us to obtain new information on the potential significance of Sr and Nd isotopes in discriminating the provenances of the siliciclastic sediment fractions delivered to the Pacific Ocean and to characterize the seasonal-scale climatic controls on the sediment inputs to the Benham Rise. In addition, analyses of the Nd isotopic compositions conducted on the planktonic foraminifera collected within the water column at different depths permit us to assess for the first time the evolution of foraminiferal ε_{Nd} values during their settling in the ocean in the context of strong seasonal variations in lithogenic inputs.

2. Materials and Methods

A mooring system with two time series sediment traps (PARFLUX Mark 78HW units, each of which has a coverage area of 0.5 m^2 and 21 sampling cups; USA) was deployed at site T1 (15°58′N, 124°41′E; water depth of 3,037 m) on the Benham Rise in the western Philippine Sea at water depths of 500 and 2,800 m from 15 January to 21 December 2015 (Figure 1). Each sampling cup was filled with 5% formaldehyde to prevent biological degradation of the sampled particulates. In total, 33 modern samples were collected at equal 20-day intervals. Of these samples, 17 were collected at a water depth of 500 m and 16 samples were collected at a water depth of 2,800 m; one sample collected between 25 June and 14 July was lost during the recovery process. The trapping efficiency of the sediment traps was guaranteed by the low tilt magnitude ($<3°$ from the vertical). In addition, two recording current meters (SEAGUARD Intermediate Water and SEAGUARD Deep Water; Norway) together with conductivity-temperature-depth sensors (4,319, 4,060, and 4,117; Norway) were closely attached to these sediment traps to collect the relevant hydrographic parameters of the intermediate and deepwater masses at intervals of 10 min.

The Sr and Nd isotopic compositions of the siliciclastic fractions of 15 of the sediment trap samples were measured following the pretreatment procedure described in detail by Xu et al. (2015). Most of the samples analyzed in this way were collected at a water depth of 2,800 m because of the limited amount of sample material recovered at a water depth of 500 m. In brief, the samples were treated with deionized water, 10% HOAc, a mixture of 1-mol/L $NH_2 \cdot OH \cdot HCl$ and 25% HOAc, 5% H_2O_2, and 2-mol/L Na_2CO_3 to remove sea salt, calcium carbonate, authigenic components, organic compounds, and biogenic silica, respectively. The remaining siliciclastic sediment fractions were dissolved in HF-$HClO_4$ and HNO_3-HCl mixtures. An initial chemical separation of Sr and rare earth elements was carried out using Biorad® columns packed with AG50W-X8, 200–400 mesh cationic exchange resin, following the procedure described in detail by Colin et al. (1999). The Sr fraction was purified using a 20-μl Sr Spec column consisting of a polyethylene syringe with a 4-mm Ø Millex filter. The Nd was then extracted and purified from the rare earth element fractions using an Eichrom® Ln Spec resin column (Copard et al., 2010).

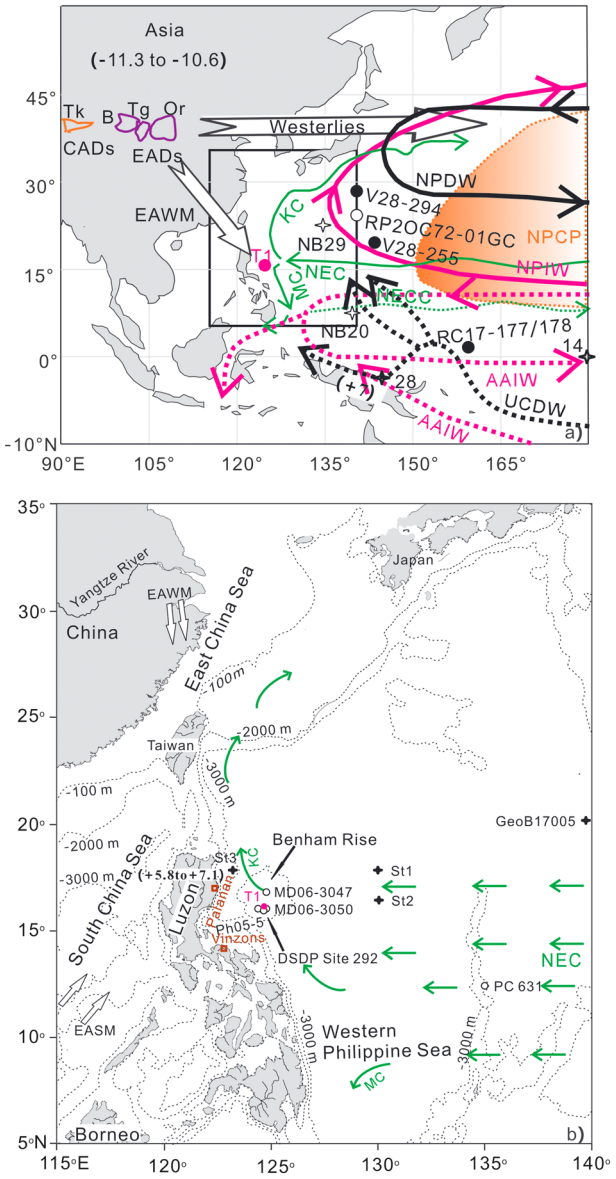

Figure 1. Maps showing the locations of the sediment trap site T1 (solid circle in a); the seawater sites GeoB17005 (Behrens et al., 2018) in addition to St1, St2, and St3 (solid pluses in b; Wu et al., 2015) and 14 and 28 (solid pluses in a; Jeandel et al., 2013); the fossil fish teeth/debris sites NB29 and NB20 (hollow pluses in a; Horikawa et al., 2011); the foraminifer sites RC17–177, RC17–178, V28–255, and V28–294 (solid circles in a; Hu et al., 2016); the sediment cores MD06–3047 (Xu et al., 2015), Deep Sea Drilling Project (DSDP) site 292 (Hickey-Vargas, 1991), MD06–3050 (Yu et al., 2016), Ph05–5 (Jiang et al., 2016), PC631 (hollow circles in b; Seo et al., 2014), and RP2OC72-01GC (hollow circle in a; Pettke et al., 2002); the weather stations Palanan and Vinzons (hollow squares in b) in the Philippine Sea and nearby regions. The rectangle part of (a) is enlarged in (b). The −100, −2,000, and −3,000-m isobaths are shown as dotted lines in (b). Also shown are the major rivers, the modern circulation patterns (the green, pink, and black arrows show the surface, intermediate, and deep currents, respectively; these paths are modified from Wu et al., 2015 and Behrens et al., 2018), the monsoon directions (white arrows), and the ε_{Nd} values (bold numbers) of the siliciclastic sediment fractions in the potential source areas (Chen et al., 2007; Defant et al., 1990; Goldstein & Jacobsen, 1988; Jeandel et al., 2013). Note that the two major drivers of eolian transport from mainland Asia to the Pacific Ocean are suggested to be the westerlies and the East Asian winter monsoon (EAWM; Seo et al., 2014; Shao et al., 2011), and the two corresponding deposition centers are the North Pacific central province and the southern part of North Pacific margin province (core RP2OC72-01GC in the Philippine Sea) in (a) (Pettke et al., 2002). The eastern Asian deserts, including the Tengger/Badain Jaran (b) and the Ordos (Or) Deserts, and the central Asian deserts, including the Taklimakan Desert, are indicated by purple and orange polygons, respectively, in (a). EASM: East Asian summer monsoon, NEC: North Equatorial Current, KC: Kuroshio Current, MC: Mindanao Current, NECC: North Equatorial Countercurrent, NPIW: North Pacific Intermediate Water, AAIW: Antarctic Intermediate Water, NPDW: North Pacific Deep Water, UCDW: Upper Circumpolar Deep Water.

Approximately 50–60 mg of well-preserved planktonic foraminifera (*Globigerinoides ruber* and *Globigerinoides sacculifer*) were picked by hand from the >150-μm fractions for the Nd isotopic analysis. In total, two samples collected at a water depth of 500 m during the autumn and winter as well as three samples collected at a water depth of 2,800 m during the summer, autumn, and winter were analyzed. The pretreatment procedure is described in detail by Wu et al. (2017). In brief, the planktonic foraminifera were gently crushed and sonicated in an ultrasonic bath to remove particulates. The clay-free foraminifera were subsequently leached in dilute acid (0.0001-mol/L HNO_3) in an ultrasonic bath. After the cleaning step, the samples were then dissolved in 0.5-mol/L HNO_3 until complete dissolution was reached. The supernatant was immediately transferred to Teflon beakers after the centrifugation of the dissolved foraminifera. Then, Nd purification was performed for all samples using TRU Spec and Ln Spec resins, following the analytical procedure described in detail by Copard et al. (2010).

The Sr and Nd isotopic compositions of all of the purified Sr and Nd fractions were measured using a Thermo Scientific NEPTUNE^{Plus} Multi-Collector Inductively Coupled Plasma Mass Spectrometer at the Laboratoire des Sciences du Climat et de l'Environnement in Gif-sur-Yvette (France). The solutions were analyzed at concentrations ranging from 15 to 20 ng/g. The mass-fractionation correction was made by normalizing $^{86}Sr/^{88}Sr$ to 0.1194 and $^{146}Nd/^{144}Nd$ to 0.7219 and applying an exponential-fractionation correction. During the analysis, every two samples were bracketed with analyses of an appropriate Sr standard solution (NIST SRM987) characterized by a certified value of 0.71025 (Weis et al., 2006). Long-term repeated analysis of NIST SRM987 gave a mean $^{87}Sr/^{86}Sr$ value of 0.71024 ± 0.00001 (2σ; Colin et al., 2010). For the Nd isotopic composition analyses, the samples were bracketed with analyses of Nd standard solutions (JNdi-1 and La Jolla) with concentrations similar to those of the samples (which ranged from 15 to 20 ng/g) and characterized by certified values of 0.512115 ± 0.000006 (Tanaka et al., 2000) and 0.511858 ± 0.000007 (Lugmair et al., 1983), respectively. The analytical uncertainty was taken to be the reproducibility (2σ) of the La Jolla standard for the individual measurement sessions (approximately 0.3 epsilon units). The total blank values were <20 pg, which can be considered negligible, for both analytical procedures used. Details regarding the quantitative calculation of the fluxes and percentages of eolian dust and volcanic materials deposited on the Benham Rise, western Philippine Sea, based on the Sr-Nd isotopic compositions of siliciclastic sediment fractions were reported previously by Xu et al. (2015).

3. Results

3.1. Siliciclastic Sediment Fractions

The mass fluxes of the different sediment fractions derived from the samples collected in this study together with the $^{87}Sr/^{86}Sr$ ratios and the ε_{Nd} values obtained from the siliciclastic sediment fractions are reported in Table 1 and Figure 2. The mass fluxes of the total particulates (which range from 10.5 to 163.0 mg/m^2/d with a mean value of 67.1 mg/m^2/d) and of the total siliciclastic sediment fractions (which range from 1.3 to 92.1 mg/m^2/d with a mean value of 31.0 mg/m^2/d) at a water depth of 2,800 m display seasonal variability. The highest fluxes for the samples collected at this water depth correspond to the periods extending from January to March 2015 and between November and December 2015, during which the fluxes of the total particulates ranged from 102.0 to 163.0 mg/m^2/d and from 45.1 to 82.2 mg/m^2/d and the fluxes of the total siliciclastic sediment fractions ranged from 56.2 to 92.1 mg/m^2/d and from 21.6 to 39.5 mg/m^2/d, respectively. Such variation trends are also seen in the mass fluxes of the total particulates at a water depth of 500 m ranging from 9.3 to 63.1 mg/m^2/d (averaging 25.6 mg/m^2/d) with the highest values occurring between January and March 2015 (which range from 30.7 to 63.1 mg/m^2/d with a mean value of 40.9 mg/m^2/d) as well as between November and December 2015 (which range from 20.2 to 40.8 mg/m^2/d with a mean value of 30.4 mg/m^2/d). Their close correspondence is documented by the high correlation coefficient (R = 0.84) between the mass fluxes of the total particulates at water depths of 500 and 2,800 m. The above variations in the mass fluxes are also associated with seasonal changes in the ε_{Nd} values (which range from −8.2 to −2.4 with a mean value of −4.9) and the $^{87}Sr/^{86}Sr$ ratios (which range from 0.70627 to 0.70798 with a mean value of 0.70708). The samples collected at a water depth of 2,800 m from April to October 2015 are characterized by lower ε_{Nd} values (which range from −6.7 to −4.9) and higher $^{87}Sr/^{86}Sr$ ratios (which range from 0.70720 to 0.70798) than those collected from January to March 2015 (which have ε_{Nd} values that range from −3.3 to −2.4 and $^{87}Sr/^{86}Sr$ ratios that range from 0.70640 to 0.70649), as well as

Table 1
The Sr and Nd Isotopic Compositions, the Contribution Percentages, and the Mass Fluxes of the Potential Source Areas of Particulate Matter Settling to Water Depths of 500 m (U) and 2,800 m (D) at Site T1 in the Western Philippine Sea

Sample no.	Period (2015)	$^{87}Sr/^{86}Sr$	SD (2σ)	$^{143}Nd/^{144}Nd$	SD (2σ)	ε_{Nd}	SD (2σ)	Dust (%)*	Volcanic (%)*	Mass flux (mg/m^2/d)			
										Total	Siliciclastic	Dust	Volcanic
U2	2/5–2/24	0.70768	0.00001	0.512218	0.000018	−8.2	0.3	62.6	37.4	10.5	1.3	0.8	0.5
D1	1/15–2/4	0.70640	0.00002	–	–	–	–	–	–	163.0	92.1	–	–
D2	2/5–2/24	0.70645	0.00002	0.512514	0.000018	−2.4	0.3	33.8	66.2	152.3	92.1	31.1	61.0
D3	2/25–3/16	0.70649	0.00002	0.512504	0.000017	−2.6	0.3	34.8	65.2	145.2	83.3	29.0	54.3
D4	3/17–4/5	0.70644	0.00002	0.512469	0.000018	−3.3	0.3	37.8	62.2	102.0	56.2	21.3	35.0
D5	4/6–4/25	0.70720	0.00001	0.512389	0.000018	−4.9	0.3	45.1	54.9	37.3	16.3	7.3	8.9
D6	4/26–5/15	0.70778	0.00002	0.512327	0.000018	−6.1	0.3	51.2	48.8	41.2	12.1	6.2	5.9
D7	5/16–6/4	0.70761	0.00002	0.512327	0.000018	−6.1	0.3	51.3	48.7	26.6	8.3	4.3	4.1
D8	6/5–6/24	0.70722	0.00002	0.512335	0.000017	−5.9	0.3	50.5	49.5	48.5	13.2	6.7	6.6
D10	7/15–8/3	0.70740	0.00002	0.512352	0.000017	−5.6	0.3	48.8	51.2	80.9	24.2	11.8	12.4
D11	8/4–8/23	0.70798	0.00001	0.512295	0.000018	−6.7	0.3	54.5	45.5	37.5	8.6	4.7	3.9
D12	8/24–9/12	–	–	–	–	–	–	–	–	32.9	4.7	–	–
D13	9/13–10/2	0.70798	0.00002	0.512329	0.000018	−6.0	0.3	51.0	49.0	29.3	10.1	5.2	5.0
D14	10/3–10/22	–	–	–	–	–	–	–	–	32.7	8.5	–	–
D15	10/23–11/11	0.70627	0.00001	0.512475	0.000018	−3.2	0.3	37.4	62.6	45.1	21.6	8.1	13.5
D16	11/12–12/1	0.70648	0.00002	0.512458	0.000018	−3.5	0.3	38.7	61.3	73.4	35.4	13.7	21.7
D17	12/2–12/21	0.70675	0.00002	0.512456	0.000018	−3.5	0.3	39.0	61.0	82.2	39.5	15.4	24.1

Note. SD: standard deviation, −: not determined, *: percentage of the siliciclastic sediment fractions.

those collected from November to December 2015 (which have ε_{Nd} values that range from −3.5 to −3.2 and $^{87}Sr/^{86}Sr$ ratios that range from 0.70627 to 0.70675; Table 1 and Figure 2).

3.2. Planktonic Foraminifera

The ε_{Nd} values obtained from well-preserved planktonic foraminifera (*G. ruber* and *G. sacculifer*) collected at water depths of 500 and 2,800 m are reported in Table 2. They are characterized by within error identical ε_{Nd} values (−3.4 ± 0.3 and −3.0 ± 0.3) at a water depth of 500 m and by a small variation of ε_{Nd} values (which range from −1.9 ± 0.3 to −0.9 ± 0.3) at a water depth of 2,800 m; the average values at these depths are −3.2 and −1.4, respectively (Table 2).

Furthermore, the ε_{Nd} values of the planktonic foraminifera collected at a water depth of 500 m display no hint of seasonal oscillation (Table 2). In contrast, the ε_{Nd} values of the planktonic foraminifera collected at a water depth of 2,800 m indicate some seasonal variability; the highest value occurs in the winter (−0.9 ± 0.3), followed by that in the autumn (−1.4 ± 0.3), and the lowest value occurs in the summer (−1.9 ± 0.3; Table 2). However, further measurements are necessary to confirm such seasonal variation trends in the future.

4. Discussion

4.1. Provenances and Fluxes of the Siliciclastic Sediment Fractions

To further discriminate the spatial and temporal changes in the inputs and fluxes of the siliciclastic sediment fractions to the western Philippine Sea, the $^{87}Sr/^{86}Sr$ ratios and the ε_{Nd} values obtained from the modern sediment trap samples are plotted on an $^{87}Sr/^{86}Sr$ versus ε_{Nd} diagram together with those previously obtained from sediments from core MD06–3047 located in the western Philippine Sea (Xu et al., 2015) and core PC631 located in the central Philippine Sea (Figure 3; Seo et al., 2014).

The provenances of siliciclastic sediments delivered to the Philippine Sea have been investigated previously in several studies, but this topic is still under debate (Jiang et al., 2013, 2016; Seo et al., 2014). The sediment inputs to site T1 located above the Benham Rise have been effectively demonstrated to represent a mixing of two end-members, namely, eolian dust from Asia and fluvial sediments from Luzon Island (Jiang et al., 2013, 2016; Xu et al., 2015; Yu et al., 2016). The Sr and Nd isotopic compositions of Luzon Island bedrock are well defined by relatively homogeneous $^{87}Sr/^{86}Sr$ ratios (which range from 0.70366 to 0.70524) and ε_{Nd} values (which range from +5.8 to +7.1; Defant et al., 1990; Goldstein & Jacobsen, 1988; Liu et al., 2016). The Sr and

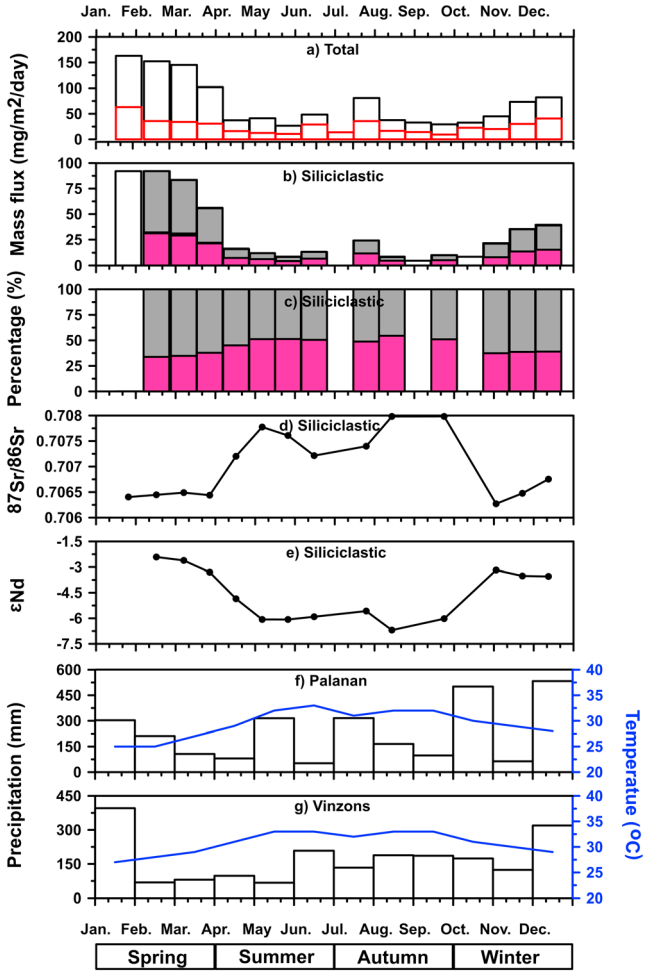

Figure 2. Temporal changes in the mass fluxes of (a) the total particulate matter and (b) the total siliciclastic sediment fractions, including eolian dust (pink shading) and volcanic materials (gray shading), as well as the percentages of (c) eolian dust (pink shading) and volcanic materials (gray shading) collected at water depths of 500 m (red lines) and 2,800 m (black lines) at site T1 during different seasons. (d) The $^{87}Sr/^{86}Sr$ ratios of the total siliciclastic sediment fractions, (e) the ε_{Nd} values of the total siliciclastic sediment fractions collected at a water depth of 2,800 m at site T1 during different seasons, (f) the precipitation and temperature at Palanan (http://www.worldweatheronline.com), and (g) the precipitation and temperature at Vinzons on eastern Luzon Island (http://www.worldweatheronline.com) are also shown.

Nd isotopic compositions of <5-μm eolian dust collected from the Taklimakan Desert (which has $^{87}Sr/^{86}Sr$ ratios that range from 0.72682 to 0.73018 and ε_{Nd} values that range from −10.7 to −10.3), the Tengger/Badain Jaran Deserts (which has $^{87}Sr/^{86}Sr$ ratios that range from 0.72919 to 0.73218 and ε_{Nd} values that range from −11.9 to −8.3), and the Ordos Desert (which has $^{87}Sr/^{86}Sr$ ratios that range from 0.72114 to 0.72419 and ε_{Nd} values that range from −17.7 to −11.5) are well known to represent eolian dust from mainland Asia (Chen et al., 2007; Seo et al., 2014). As shown in Figure 3a, the Sr and Nd isotopic signatures of the modern sediment trap samples and those of the sediments extracted from the nearby cores MD06–3047 and PC631 (Figure 1) that were deposited after the mid-Quaternary (Seo et al., 2014; Xu et al., 2015) fall on a mixing line between the two end-members, which correspond to eolian dust derived from mainland Asia and the volcanic province of Luzon Island. The $^{87}Sr/^{86}Sr$ versus ε_{Nd} diagram permits us to quantitatively discriminate the contributions of eolian dust from the Ordos Desert from those from the Taklimakan and the Tengger/Badain Jaran Deserts (Figure 3a). In greater detail, all of the results presented in this study plot close to the mixing curve between Luzon Island and the Ordos Desert (Figure 3), suggesting the mixing of sediments derived from the volcanic province of Luzon Island and dust originating predominantly from the Ordos Desert. In Figure 3b, we display different mixing curves between Luzon Island material and several proportions of dust from both the Taklimakan Desert (20%, 40%, and 60%) and the Ordos Desert (80%, 60%, and 40%) for comparison. This procedure indicates that eolian dust from the Ordos Desert represents an excess of 80% of the modern eolian deposition at site T1.

Similar results were obtained from the Quaternary sediments from core MD06–3047 (Xu et al., 2015), which is located in the western Philippine Sea (Figure 1). This result suggests that the EAWM may be associated with a dominant proportion of eolian dust derived from the Ordos Desert (generally >80%; Figure 3b) within the study area. In addition, the Quaternary sediments from core PC631, which is located in the southeastern part of the central Philippine Sea (Figure 1), also fall between the two mixing lines reported in Figure 3a; this result also suggests a dominant contribution from the Ordos Desert (generally >80%) to the eolian deposition therein and a relatively low proportion of volcanic matter, which is in agreement with the distal location of this core relative to the volcanic province of Luzon Island (Figure 1). All of the results obtained from these marine core sediments compare well with those of the sediment trap samples, and these results indicate that the Ordos Desert has been the predominant

Table 2
The Nd Isotopic Compositions of the Planktonic Foraminifera Settling to Water Depths of 500 and 2,800 m at Site T1 in the Western Philippine Sea

Water depth (m)	Sample no.	Period (2015)	Season (2015)	$^{143}Nd/^{144}Nd$	SD (2σ)	ε_{Nd}	SD (2σ)
500	U10	7/15–8/3	Autumn	0.512465	0.000018	−3.4	0.3
500	U15	10/23–11/11	Winter	0.512484	0.000018	−3.0	0.3
2,800	D8	6/5–6/24	Summer	0.512541	0.000018	−1.9	0.3
2,800	D12	8/24–9/12	Autumn	0.512564	0.000018	−1.4	0.3
2,800	D15	10/23–11/11	Winter	0.512593	0.000018	−0.9	0.3

Note. SD: standard deviation.

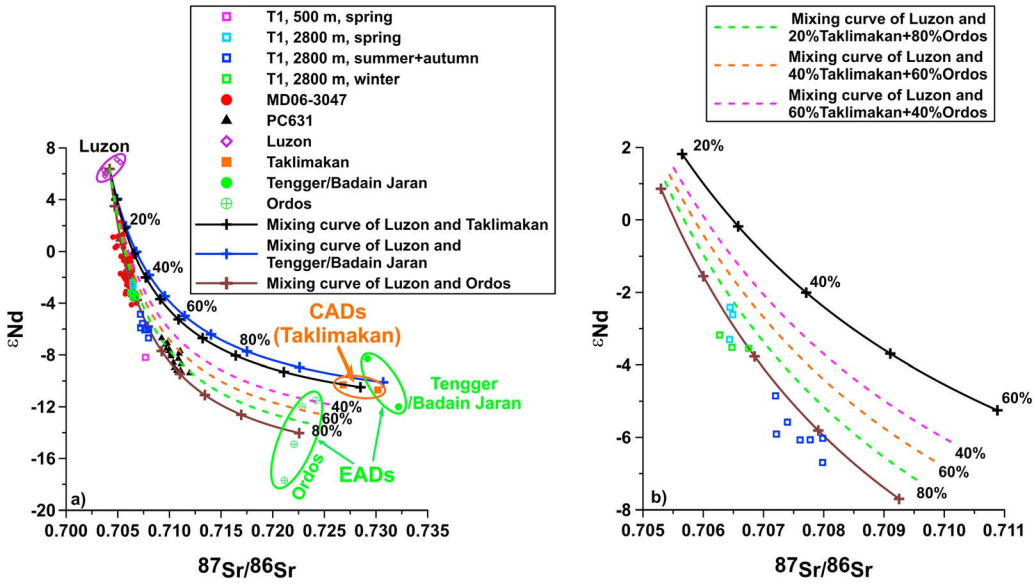

Figure 3. Discrimination plot showing (a) the variations in the $^{87}Sr/^{86}Sr$ ratios and ε_{Nd} values of the siliciclastic sediment fractions from site T1 as well as cores MD06–3047 (Xu et al., 2015) and PC631 (Seo et al., 2014). For comparison, the Sr and Nd isotopic data of the potential source areas, including Luzon Island (Defant et al., 1990; Goldstein & Jacobsen, 1988) and the Taklimakan, the Tengger/Badain Jaran, and the Ordos Deserts (Chen et al., 2007), are also plotted. The mixing curves between Luzon Island and the Taklimakan Desert, between Luzon Island and the Tengger/Badain Jaran Deserts, and between Luzon Island and the Ordos Desert are calculated using the method of Jiang et al. (2013). The mixing curves between Luzon Island and the Taklimakan Desert (20%, 40%, and 60% contributions) plus the Ordos Desert (80%, 60%, and 40% contributions) calculated using the method of Jiang et al. (2013) are also shown. Furthermore, the key part of (a) concerning the study samples is enlarged in (b). The concentrations of Sr and Nd and the isotopic compositions used here are Sr = 439.5 μg/g, Nd = 19.1 μg/g, $^{87}Sr/^{86}Sr$ = 0.70421, and ε_{Nd} = +6.4 for average volcanic materials from Luzon Island (Defant et al., 1990; Goldstein & Jacobsen, 1988); Sr = 111.0 μg/g, Nd = 28.3 μg/g, $^{87}Sr/^{86}Sr$ = 0.72850, and ε_{Nd} = −10.5 for average eolian dust from the Taklimakan Desert (Chen et al., 2007); Sr = 111.0 μg/g, Nd = 28.3 μg/g, $^{87}Sr/^{86}Sr$ = 0.73069, and ε_{Nd} = −10.1 for average eolian dust from the Tengger/Badain Jaran Deserts (Chen et al., 2007); and Sr = 111.0 μg/g, Nd = 28.3 μg/g, $^{87}Sr/^{86}Sr$ = 0.72256, and ε_{Nd} = −14.0 for average eolian dust from the Ordos Desert (Chen et al., 2007).

contributor of eolian dust to the Philippine Sea since at least 600 ka (Xu et al., 2015); this is because the eolian dust samples since 0.1 Ma collected from the Taklimakan, Badain Jaran, and Tengger Deserts and the North Pacific central province (Figure 1) display similar Hf-Nd isotopic values and the eolian dust from these deserts is likely transported to the northern Pacific Ocean mainly by the westerlies (Pettke et al., 2002; Zhao et al., 2014). However, dust derived from the Ordos Desert is likely transported to the southern part of the North Pacific margin province (i.e., the Philippine Sea) by the EAWM (Zhao et al., 2014).

According to the mixing curve between Luzon Island volcanic material and Ordos Desert dust, the contributions from the Ordos Desert dust to the total siliciclastic sediment fractions collected at a water depth of 2,800 m (237 m above the sea bottom) are between 33.8% and 54.5% (Figure 3a and Table 1). These values fall within the ranges derived from the Sr and Nd isotopes of siliciclastic sediments in the nearby cores MD06–3047 (between ~15% and ~50%; Xu et al., 2015) and Ph05–5 (between ~10% and ~50%; Jiang et al., 2013). A previous analysis of the backward trajectories of eolian particulate matter transported at altitudes of 100, 500, and 1,000 m above the Benham Rise (Figure 1) during a major dust event in spring 2006 clearly showed that the relevant air masses can be traced back to the eastern Asian continent, confirming that the eolian dust originated from the Ordos Desert (Jiang et al., 2013). Consequently, we conclude that the sampled eolian dust deposited in the western Philippine Sea and the central Philippine Sea throughout the middle to late Quaternary was likely derived mainly from the EADs (i.e., the Ordos Desert). This conclusion is consistent with the general concept that EAD dust is predominantly carried by northwesterly surface winds associated with the EAWM (Shao et al., 2011). Thus, sediment cores obtained from the Philippine Sea have the potential to yield continuous reconstructions of the climatic evolution of eastern Asia. This variability can then be compared with that of central Asia, which is the main source of dust for the North Pacific central province (Zhao et al., 2014).

Taking into consideration the siliciclastic sediment fluxes (Figure 2b) and our estimates of the relative proportions of eolian dust and volcanic materials from Luzon Island (Figure 3a), we estimate the variability in the fluxes of eolian dust and volcanic materials to the study area over time (Figure 2b). The mass fluxes of the total particulates, the total siliciclastic sediment fractions, the eolian dust, and Luzon volcanic sediments display similar seasonal variations at water depths of both 500 and 2,800 m during 2015; the highest values occur during the spring and winter, and the lowest values occur during the summer and autumn (Figures 2a and 2b). The increases in the fluxes of Luzon volcanic matter to the western Philippine Sea during the spring and winter of 2015 reflect greater inputs of sediments derived from heavy precipitation on eastern Luzon Island (e.g., Palanan and Vinzons, Figures 1, 2f, and 2g). Variations in the fluxes of EAD dust that are similar to those of Luzon volcanic matter indicate an enhanced EAWM during the spring and winter (http://www.worldweatheronline.com). Although the mass fluxes of both eolian dust and volcanic materials increase during the spring and winter (Figure 2b), the Sr and Nd isotopic compositions of the total siliciclastic sediment fractions deposited in these seasons are less radiogenic in Sr and more radiogenic in Nd (Figures 2d and 2e), indicating predominant contributions from Luzon Island volcanic matter (Figure 3a). In contrast, the Sr and Nd isotopic signatures indicate increased dust contributions (Figures 2d and 2e) during the summer and autumn; during these seasons, the volcanic inputs decrease drastically (Figure 2b), leading to a slight increase in the relative proportion of the dust component, even though the eolian dust fluxes also decrease during this interval (Figure 2b).

The volcanic matter is derived primarily from the weathering and erosion of volcanic bedrock on Luzon Island (Xu et al., 2015) and is transported to the study area by eastward-flowing surface and/or deep currents, which are ultimately controlled by East Asian summer monsoon (EASM) precipitation (Kawabe et al., 2009; Yu et al., 2016). In contrast, the eolian dust is mainly derived from the EADs and is transported to the Benham Rise by wind systems associated with the EAWM (Xu et al., 2015; Yu et al., 2016). As a result, the effects of the climate on the precipitation, wind intensity, and wind-driven surface currents also affect the supplies of volcanic and eolian particulates to the western Philippine Sea (Xu et al., 2015; Yu et al., 2016). The generally reduced precipitation over eastern Luzon Island (Figures 2f and 2g) and the weaker EAWM intensity in the winter of 2015 likely accounted for the lower mass fluxes of the total particulates, Luzon volcanic matter, and EAD dust to the Philippine Sea during the winter than during the spring, possibly at water depths of both 500 and 2,800 m. Such close correlations between the weakened summer monsoonal precipitation over eastern Luzon Island and the lower inputs of local volcanic erosion/weathering products to the western Philippine Sea and between the decreased EAWM intensity in eastern Asia and the smaller eolian dust contribution to the sea during the geological past are also recorded in cores MD06–3047, MD06–3050, and Ph05–5 (Figure 1) collected from the study area. In addition, eastward-flowing deep currents, including the Upper Circumpolar Deep Water (UCDW) and the North Pacific Deep Water (NPDW) near the Philippine Sea, have been observed instrumentally by Kawabe et al. (2009). The relatively strong eastward movement of warm surface waters from the western Pacific Warm Pool (including the study area) to the eastern Pacific Ocean and the eastward-flowing deep currents (Kawabe et al., 2009) passing over the study site in the winter of 2015 (for more details, see section 4.2) may also be responsible for the reduced mass flux of volcanic matter from eastern Luzon Island to the study area. Under such conditions, some volcanic particulate matter derived from Luzon Island may be further transported to the central Philippine Sea by the eastward-flowing surface and/or deep currents (Seo et al., 2014). Furthermore, the presence of dust emissions in the source region that are weaker during the winter than during the spring may partly account for the lower mass flux of eolian dust at the study site during the winter. The results of this study therefore confirm the close link between the monsoonal precipitation on eastern Luzon Island, the EAWM intensity in eastern Asia, and the siliciclastic deposition in the western Philippine Sea both during the present-day and during the Quaternary (Jiang et al., 2016; Xu et al., 2015; Yu et al., 2016).

4.2. Significance of the Seasonal Variations in Foraminiferal ε_{Nd} Values Within the Water Column

The ε_{Nd} values of two planktonic foraminiferal samples collected at a water depth of 500 m at site T1 in the autumn and winter of 2015 are characterized by within error identical ε_{Nd} values of -3.4 ± 0.3 and -3.0 ± 0.3 (Table 2). These values are also similar (within analytical error) to those of seawater collected at the same water depth at nearby sites St1 (-3.4 ± 0.3; Figures 1 and 4) and St2 (-2.8 ± 0.3; Figures 1 and 4) in the winter of 2010 (Wu et al., 2015) as well as site GeoB17005 (-3.2 ± 0.4; Figures 1 and 4) in the winter of 2012 (Behrens et al., 2018). These results indicate that the ε_{Nd} values of planktonic foraminifera obtained from the intermediate

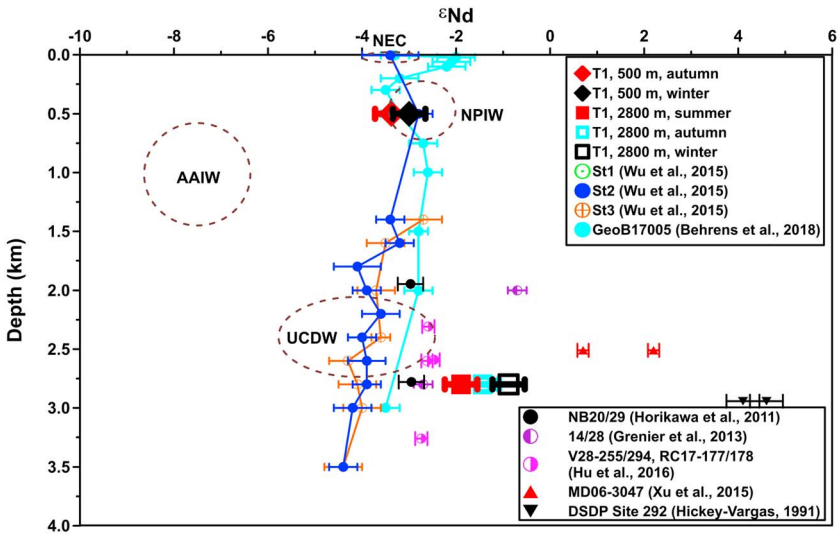

Figure 4. Comparison of seawater ε_{Nd} values derived from this study with previously published data obtained at nearby sites (Behrens et al., 2018; Grenier et al., 2013; Horikawa et al., 2011; Hu et al., 2016; Wu et al., 2015). The ranges for the potential water masses, including the Antarctic Intermediate Water, the North Pacific Intermediate Water, and the Upper Circumpolar Deep Water, are modified from Wu et al. (2015). The ε_{Nd} values of core-top sediments (Xu et al., 2015) and volcanic basement rocks (Hickey-Vargas, 1991) in the study area are also shown for comparison.

seawater collected at site T1 in different seasons are homogeneous and are not strongly modified by obviously seasonal changes in lithogenic inputs to the water column, including eolian dust and volcanic matter (Figures 2 and 4). In addition, the ε_{Nd} values measured in seawater and planktonic foraminifera collected at different locations (Figure 1) and in different seasons (i.e., winter 2010, winter 2012, autumn 2015, and winter 2015) suggest that the provenance and mixing proportions of the water masses were similar over this period (Figure 4). These ε_{Nd} values are similar to those of the North Pacific Intermediate Water (NPIW) at sites BO-5 (20°0.0′N, 175°0.0′W; Amakawa et al., 2009) and TPS24 271–1 (24°17.2′N, 150°28.2′E; Piepgras & Jacobsen, 1988) in the subtropical gyre of the northern Pacific Ocean ranging from -4.2 ± 0.6 to -2.7 ± 0.3 and from -3.8 ± 0.3 to -2.9 ± 0.3, respectively. These results confirm that the intermediate water masses at site T1 are likely strongly influenced by NPIW being advected from the north (Wu et al., 2015).

These two planktonic foraminiferal ε_{Nd} values collected at a water depth of 500 m at the study site in different seasons of 2015 are identical (within analytical error) to those of surface seawater at nearby sites St2 (-3.4 ± 0.6; Figures 1 and 4) in the winter of 2010 (Wu et al., 2015) and GeoB17005 (-3.3 ± 0.3; Figures 1 and 4) in the winter of 2012 (Behrens et al., 2018). *G. ruber* and *G. sacculifer* originally live at shallow water depths (20–50 m) and then sink to the studied water depths of 500 and 2,800 m when they are dead. Thus, the studied planktonic foraminiferal ε_{Nd} values collected at a water depth of 500 m may be expected to record the surface seawater ε_{Nd} characteristics. Once again, the homogeneous planktonic foraminiferal ε_{Nd} values obtained from both the surface and the intermediate seawater at different locations (Figure 1) and in different seasons (i.e., winter 2010, winter 2012, autumn 2015, and winter 2015) may indicate a similar provenance of the surface water masses (i.e., the North Equatorial Current (NEC) with ε_{Nd} values of ~-3) and may reveal the nonsignificant influences of obviously seasonal changes in the lithogenic inputs to the water column throughout the study area over this period (Figures 2 and 4; Behrens et al., 2018; Wu et al., 2015). Unfortunately, the similar ε_{Nd} values of the NEC and the NPIW in the study area (Behrens et al., 2018; Wu et al., 2015) do not permit further discrimination between the respective significances of these two potential source water masses on the study planktonic foraminiferal Nd isotopic characteristics here. However, such modern results may shed light on interpretations of Nd isotopic compositions analyzed on paleoclimatic archives and thus significantly improve our knowledge of the Nd cycle as well as surface/intermediate water circulation in the Kuroshio source region during the geological past (Hu et al., 2016).

In addition, the ε_{Nd} values obtained from three planktonic foraminiferal samples collected at a water depth of 2,800 m indicate a small seasonal variability; the ε_{Nd} values in the summer, autumn, and winter of 2015 are

−1.9 ± 0.3, −1.4 ± 0.3, and −0.9 ± 0.3, respectively (Table 2). These ε_{Nd} values systematically reflect more radiogenic material than those obtained from planktonic foraminiferal samples collected at a water depth of 500 m in the autumn and winter of 2015 (−3.4 ± 0.3 and −3.0 ± 0.3, respectively; Figure 4). These results indicate significant modification of the Nd isotopic compositions of planktonic foraminifera during their settling within the water column. A previous study demonstrated that the Nd concentrations of dead planktonic foraminifera increase in the water column due to the precipitation of secondary Mn coatings, which suggests a possible major disturbance of the primary Nd isotopic compositions acquired at the surface of the ocean (Pomiès et al., 2002). Our results indicate that the primary foraminiferal ε_{Nd} values acquired at the surface may be modified rapidly within the water column, potentially due to the precipitation of secondary Mn coatings. Unfortunately, Nd and Mn concentrations have not been measured within samples of planktonic foraminifera to further confirm this hypothesis.

However, the ε_{Nd} values obtained from foraminifera collected at a water depth of 2,800 m (which range from −1.9 ± 0.3 to −0.9 ± 0.3) are clearly different from the ε_{Nd} values for the NPDW in the Pacific Ocean (which range from −4 to −3.5), the northern Pacific Ocean (which range from −6 to −4), the Philippine Sea (which range from −4.4 to −3.0), and the northwestern Pacific Ocean (−4; Horikawa et al., 2011; Wu et al., 2015, and references therein; Hu et al., 2016, and references therein). According to the most recent study on dissolved Nd isotopes in the study area and adjacent regions, the NPDW is apparently located too far away in the northeast of the sampling location to influence the study area (Behrens et al., 2018). In addition, such values are significantly different from those for the UCDW in the southern Pacific Ocean (~−8), the southwestern Pacific Ocean (~−6.5), the equatorial western Pacific (~−3), and the Philippine Sea (which range from −3.0 to −2.8; Wu et al., 2015, and references therein; Hu et al., 2016, and references therein; Behrens et al., 2018). Considering the lack of seasonal change in the seawater ε_{Nd} values in conjunction with the very low siliciclastic ε_{Nd} value of −8.2 at a water depth of 500 m (Tables 1 and 2 as well as Figure 4), the above seasonal variations in the seawater ε_{Nd} values at a water depth of 2,800 m may not result from the dissolution effect of surface input via continental particulates (Grasse et al., 2017). In contrast, these foraminiferal ε_{Nd} values are close to those of the deepwater masses (which range from −2.5 to −0.5) obtained near the radiogenic (approximately +7) volcanic margin of the western Pacific Ocean farther south and along the pathway of the modified UCDW, which may reach the southern Philippine Sea (Figure 1). Close to this volcanic margin, for example, the modified UCDW is characterized by more radiogenic ε_{Nd} values that reach −0.7 ± 0.2 at site 28 (Figures 1 and 4; Grenier et al., 2013).

Furthermore, the deepwater masses at site T1 (237 m above the sea bottom) may be altered by local boundary exchange with radiogenic sediments from adjacent areas. Although few ε_{Nd} values from local sediments are available, the limited published data show that the local rocks and sediments are both characterized by radiogenic Nd isotope signatures. For example, the ε_{Nd} values of two samples of volcanic basement rock obtained at DSDP Site 292 reach +4.1 and +4.6, and those of two core-top sediment samples obtained from core MD06–3047 collected from the Benham Rise are +0.7 and +2.2 (Hickey-Vargas, 1991; Xu et al., 2015). The large differences in the ε_{Nd} values between these radiogenic rocks (which range from +4.1 to +4.6) and sediments (which range from +0.7 to +2.2) on the sea bottom and the UCDW flowing over sites St2 and St3 (−4.1 ± 0.5; Wu et al., 2015) as well as GeoB17005 (−2.8 ± 0.3; Behrens et al., 2018) permit exchange between deepwater masses and resuspended particulate matter (Grenier et al., 2013; Hu et al., 2016). As a result, the exchange in Nd between lithogenic particulates and deepwater masses observed at site T1 in the summer, autumn, and winter of 2015 has the potential to greatly modify the Nd isotopic compositions of the UCDW in the western Philippine Sea. The modified UCDW in this area is thus characterized by relatively radiogenic Nd isotopic compositions, as observed by Grenier et al. (2013) and Wu et al. (2017) in nearby regions, and it significantly alters the ε_{Nd} values of the planktonic foraminifera settling to a water depth of 2,800 m (Figure 4).

Of particular interest, the planktonic foraminiferal ε_{Nd} values obtained at a water depth of 2,800 m display seasonal changes that are characterized by an increase from −1.9 ± 0.3 in the summer to −1.4 ± 0.3 in the autumn and −0.9 ± 0.3 in the winter of 2015 (Table 2). This increase is associated with a decrease in both the deepwater temperature and the salinity from the summer to the winter through the autumn of 2015 (Figures 5c and 5d), suggesting a potentially increasing influence of another deepwater mass characterized by lower temperatures and salinities. In addition, the deep current is characterized by an absolute speed in the winter that is higher than those in the summer and autumn of 2015 (Figure 5b). As discussed above,

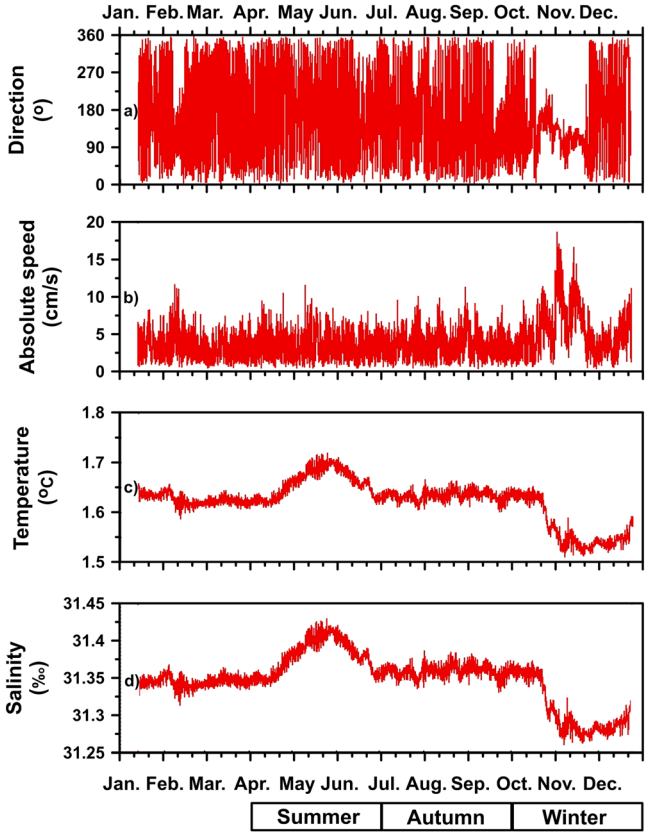

Figure 5. Temporal changes in the deep currents, including their (a) direction, (b) absolute speed, (c) temperature, and (d) salinity at a water depth of 2,800 m at intervals of 30 min (3-point running average) in 2015. Note the obvious variations in all of these parameters in the winter of 2015. Different seasons in which planktonic foraminifera were collected at the same water depth and then analyzed for the ε_{Nd} values are also shown.

the ε_{Nd} values of neither the original NPDW (which range from −4.4 to −3.0; Horikawa et al., 2011; Wu et al., 2015) nor the original UCDW (which range from −3.0 to −2.8; Behrens et al., 2018; Hu et al., 2016) that may flow into the western Philippine Sea can explain the anomalous ε_{Nd} values of the planktonic foraminifera collected at a water depth of 2,800 m that are reported in the present study. Furthermore, this current runs southeastward and has a dominant flow direction of ~120° (Figure 5a), which clearly differs from the primary flow directions of the NPDW (southward) or the UCDW (northward) that may also flow into the western Philippine Sea (Behrens et al., 2018; Hu et al., 2016; Wu et al., 2015). Given that Luzon Island is the volcanic island that lies closest to the study area to the northwest (Figure 1), and with regard to the characteristics of seawater, which includes more radiogenic Nd isotopic compositions, lower temperatures, and lower salinities, the deepwater current observed in the winter of 2015 can be derived only from the volcanic margin (e.g., the continental slope) of Luzon Island, where the ε_{Nd} values are more radiogenic (which range from +5.8 to +7.1; Defant et al., 1990; Goldstein & Jacobsen, 1988; Liu et al., 2016) and where a supply of fresh and cold water is present (Figure 1). Similar observations, including a relatively radiogenic deepwater ε_{Nd} value (−0.7 ± 0.2) collected at a similar water depth at the nearby site 28, which lies close to the coast of Papua New Guinea (Figures 1 and 4), also arise due to the strong modifying effects of the volcanic margin of Papua New Guinea, which has similarly radiogenic ε_{Nd} values (approximately +7; Grenier et al., 2013). The boundary exchange process between the deepwater mass and the radiogenic margin close to Luzon Island together with that between the deepwater and the radiogenic sediments of the Benham Rise is a critical factor that influences the Nd isotopic compositions of the deepwater masses in the western Philippine Sea. These radiogenic deepwater masses that formed in the winter of 2015 subsequently modified the ε_{Nd} values of the planktonic foraminifera settling through the water column significantly via the potential precipitation of secondary Mn coatings. Thus, the planktonic foraminifera with the highest ε_{Nd} values were collected at a water depth of 2,800 m in the winter of 2015 (Table 2).

One further explanation worth considering here is submarine groundwater discharge, which is a lower-salinity source that may significantly impact deep but not surface water in the study area (Zektser, 1996). Submarine groundwater discharge is usually enriched in rare earth elements, and it likely reflects the radiogenic ε_{Nd} values of Luzon Island (which range from +5.8 to +7.1; Defant et al., 1990; Goldstein & Jacobsen, 1988; Liu et al., 2016). Such discharge can result in radiogenic Sr (Beck et al., 2013) and increased Nd concentrations (Johannesson et al., 2011) and thus may account for the radiogenic Nd signatures in this study. In particular, seasonal changes in submarine groundwater discharge have been linked to variations in monsoonal precipitation (Hougham et al., 2008). Stronger precipitation over eastern Luzon Island in the winter than in the summer and autumn of 2015 (Figures 2f and 2g) may lead to a higher flux of submarine groundwater discharge (Hougham et al., 2008) and may result in the observed radiogenic planktonic foraminiferal ε_{Nd} values at a water depth of 2,800 m. In sum, both the boundary exchange process and submarine groundwater discharge may significantly influence the Nd isotopic compositions of the deepwater masses in the western Philippine Sea. Therefore, we should be cautious on the usage of seawater Nd isotopes as a deep circulation tracer therein.

5. Conclusions

In this study, the Sr and Nd isotopic compositions of siliciclastic fractions and the Nd isotopic compositions of planktonic foraminifera isolated from sediment trap samples in addition to high-resolution hydrographic

information (including the current direction, absolute speed, temperature, and salinity) collected at different water depths above the Benham Rise in 2015 are investigated. This investigation is carried out to track the seasonal changes in the provenances of the siliciclastic sediment fractions and the planktonic foraminiferal ε_{Nd} values throughout the water column. Moreover, the underlying mechanisms that cause these seasonal variations in the western Philippine Sea are assessed. The major conclusions are summarized below.

The siliciclastic sediment fractions obtained from the water column are derived mainly from Luzon volcanic materials (which range from 66.2% to 45.5%) and eolian dust (which range from 33.8% to 54.5%). The modern eolian dust transported to the Benham Rise is derived mainly from the EAD (>80%) and, to a lesser extent, from the Taklimakan, Badain Jaran, and Tengger Deserts (<20%). The fluxes of both Luzon volcanic matter and eolian particulate are characterized by a seasonal variability; the highest values occur in the spring, followed by those in the winter, summer, and autumn of 2015. The EASM precipitation and the EAWM intensity are the dominant controlling factors on the above changes in the mass fluxes. In addition, the planktonic foraminiferal ε_{Nd} values at water depths of 500 and 2,800 m are clearly different, and these differences indicate stratified water masses with different provenances and/or influencing factors. On the one hand, the homogeneous planktonic foraminiferal Nd isotopic compositions collected at a water depth of 500 m during the different seasons of 2015 (which range from -3.4 ± 0.3 to -3.0 ± 0.3) may suggest a negligible influence from the Nd inputs of Luzon volcanic matter and eolian dust, although these lithogenic fluxes are characterized by obvious seasonal changes. On the other hand, the ε_{Nd} values of the planktonic foraminifera collected at a water depth of 2,800 m are much higher (which range from -1.9 ± 0.3 to -0.9 ± 0.3) than those collected at a water depth of 500 m and show a hint of a seasonal increase from the summer to the winter through the autumn of 2015, possibly suggesting the rapid modification of ε_{Nd} values during the settling of planktonic foraminifera in the water column via the precipitation of secondary Mn coatings at the deposition depths of these foraminifera. However, such deductions must be confirmed with further measurements. In particular, the presence of an enhanced southeastward-flowing deep current derived from the Luzon volcanic margin in the winter of 2015 corresponds to the highest ε_{Nd} value of the planktonic foraminifera collected at a water depth of 2,800 m. These observations demonstrate the significance of the boundary exchange process, possibly that associated with the discharge of colder water (e.g., submarine groundwater) from eastern Luzon Island, in altering the Nd isotopic compositions of deepwater.

Acknowledgments
The data for this paper are available in Tables 1 and 2. We express our gratitude to the crew of R/V *Science* for collecting the sediment trap samples in the western Philippine Sea. We are grateful to Louise Bordier, Rongfang Ma, Qiong Wu, Xuebo Yin, Bingbin Qin, Mingjiang Cai, and Hongjin Chen for their considerable assistance in analyzing the samples. We also appreciate the Editors of Journal of Geophysical Research: Oceans (e.g., S. Bradley Moran) and Journal of Geophysical Research: Atmospheres (e.g., Lynn Russell) and three anonymous reviewers for their thorough and constructive comments that significantly improved the original manuscript. Financial support came from the National Programme on Global Change and Air-Sea Interaction (GASI-GEOGE-02), the Scientific and Technological Innovation Project financially supported by Qingdao National Laboratory for Marine Science and Technology (2016ASKJ13), the National Natural Science Foundation of China (41376064, 41676038, 41876034, 41230959, 41476043, and 41106043), the National Programme on Global Change and Air-Sea Interaction (GASI-GEOGE-06-04 and GASI-GEOGE-04), a part of the project titled the Study of Marine Geology and Geological Structure in the Korean Jurisdictional Sea (PM60508) funded by the Ministry of Oceans and Fisheries, Korea, the Shandong Provincial Natural Science Foundation, China (ZR2016DM12), and the Response of Marine Biotic Community Structure to Climatic Change. PC's involvement was made by the Charles T. McCord Jr. Chair in Petroleum Geology.

References

Amakawa, H., Sasaki, K., & Ebihara, M. (2009). Nd isotopic composition in the central North Pacific. *Geochimica et Cosmochimica Acta*, *70*(18), A13. https://doi.org/10.1016/j.gca.2006.06.040

Beck, A. J., Charette, M. A., Cochran, J. K., Gonneea, M. E., & Peucker-Ehrenbrink, B. (2013). Dissolved strontium in the subterranean estuary—Implications for the marine strontium isotope budget. *Geochimica et Cosmochimica Acta*, *117*, 33–52. https://doi.org/10.1016/j.gca.2013.03.021

Behrens, M. K., Pahnke, K., Schnetger, B., & Brumsack, H.-J. (2018). Sources and processes affecting the distribution of dissolved Nd isotopes and concentrations in the West Pacific. *Geochimica et Cosmochimica Acta*, *222*, 508–534. https://doi.org/10.1016/j.gca.2017.11.008

Bird, A., Stevens, T., Rittner, M., Vermeesch, P., Carter, A., Andò, S., et al. (2015). Quaternary dust source variation across the Chinese Loess Plateau. *Palaeogeography Palaeoclimatology Palaeoecology*, *435*, 254–264. https://doi.org/10.1016/j.palaeo.2015.06.024

Chen, J., Li, G. J., Yang, J. D., Rao, W. B., Lu, H. Y., Balsam, W., et al. (2007). Nd and Sr isotopic characteristics of Chinese deserts: Implications for the provenances of Asian dust. *Geochimica et Cosmochimica Acta*, *71*(15), 3904–3914. https://doi.org/10.1016/j.gca.2007.04.033

Colin, C., Frank, N., Copard, K., & Douville, E. (2010). Neodymium isotopic composition of deep-sea corals from the NE Atlantic: Implications for past hydrological changes during the Holocene. *Quaternary Science Reviews*, *29*(19-20), 2509–2517. https://doi.org/10.1016/j.quascirev.2010.05.012

Colin, C., Turpin, L., Bertaux, J., Desprairies, A., & Kissel, C. (1999). Erosional history of the Himalayan and Burman ranges during the last two glacial-interglacial cycles. *Earth and Planetary Science Letters*, *171*(4), 647–660. https://doi.org/10.1016/S0012-821X(99)00184-3

Copard, K., Colin, C., Douville, E., Freiwald, A., Gudmundsson, G., Mol, B. D., & Frank, N. (2010). Nd isotopes in deep-sea corals in the North-Eastern Atlantic. *Quaternary Science Reviews*, *29*(19-20), 2499–2508. https://doi.org/10.1016/j.quascirev.2010.05.025

Defant, M. J., Maury, R. C., Joron, J. L., Feigenson, M. D., Leterrier, J., Bellon, H., et al. (1990). The geochemistry and tectonic setting of the northern section of the Luzon arc (the Philippines and Taiwan). *Tectonophysics*, *183*(1-4), 187–205. https://doi.org/10.1016/0040-1951(90)90416-6

Goldstein, S. J., & Jacobsen, S. B. (1988). Nd and Sr isotopic systematics of river water suspended material—Implications for crustal evolution. *Earth and Planetary Science Letters*, *87*(3), 249–265. https://doi.org/10.1016/0012-821X(88)90013-1

Grasse, P., Bosse, L., Hathorne, E. C., Böning, P., Pahnke, K., & Frank, M. (2017). Short-term variability of dissolved rare earth elements and neodymium isotopes in the entire water column of the Panama Basin. *Earth and Planetary Science Letters*, *475*, 242–253. https://doi.org/10.1016/j.epsl.2017.07.022

Grenier, M., Jeandel, C., Lacan, F., Vance, D., Venchiarutti, C., Cros, A., & Cravatte, S. (2013). From the subtropics to the central equatorial Pacific Ocean: Neodymium isotopic composition and rare earth element concentration variations. *Journal of Geophysical Research: Oceans*, *118*, 592–618. https://doi.org/10.1029/2012JC008239

Hickey-Vargas, R. (1991). Isotope characteristics of submarine lavas from the Philippine Sea: Implication for the origin of arc and basin magmas of the Philippine tectonic plate. *Earth and Planetary Science Letters*, *107*(2), 290–304. https://doi.org/10.1016/0012-821X(91)90077-U

Horikawa, K., Martin, E. E., Asahara, Y., & Sagawa, T. (2011). Limits on conservative behavior of Nd isotopes in seawater assessed from analysis of fish teeth from Pacific core topes. *Earth and Planetary Science Letters*, *310*(1-2), 119–130. https://doi.org/10.1016/j.epsl.2011.07.018

Hougham, A. L., Moran, S. B., Masterson, J. P., & Kelly, R. P. (2008). Seasonal changes in submarine groundwater discharge to coastal salt ponds estimated using ^{226}Ra and ^{228}Ra as tracers. *Marine Chemistry*, *109*(3-4), 268–278. https://doi.org/10.1016/j.marchem.2007.08.001

Hu, R., Piotrowski, A. M., Bostock, H. C., Crowhurst, S., & Rennie, V. (2016). Variability of neodymium isotopes associated with planktonic foraminifera in the Pacific Ocean during the Holocene and Last Glacial Maximum. *Earth and Planetary Science Letters*, *447*, 130–138. https://doi.org/10.1016/j.epsl.2016.05.011

Jeandel, C., Delattre, H., Grenier, M., Pradoux, C., & Lacan, F. (2013). Rare earth element concentrations and Nd isotopes in the Southeast Pacific Ocean. *Geochemistry, Geophysics, Geosystems*, *14*, 328–341. https://doi.org/10.1029/2012GC004309

Jeandel, C., & Oelkers, E. H. (2015). The influence of terrigenous particulate material dissolution on ocean chemistry and global element cycles. *Chemical Geology*, *395*, 50–66. https://doi.org/10.1016/j.chemgeo.2014.12.001

Jiang, F. Q., Frank, M., Li, T. G., Chen, T.-Y., Xu, Z. K., & Li, A. C. (2013). Asian dust input in the western Philippine Sea: Evidence from radiogenic Sr and Nd isotopes. *Geochemistry, Geophysics, Geosystems*, *14*, 1538–1551. https://doi.org/10.1002/ggge.20116

Jiang, F. Q., Zhou, Y., Nan, Q. Y., Zhou, Y., Zheng, X. F., Li, T. G., et al. (2016). Contribution of Asian dust and volcanic matter to the western Philippine Sea over the last 220 kyr as inferred from grain size and Sr-Nd isotopes. *Journal of Geophysical Research: Oceans*, *121*, 6911–6928. https://doi.org/10.1002/2016JC012000

Johannesson, K. H., Chevis, D. A., Burdige, D. J., Cable, J. E., Martin, J. B., & Roy, M. (2011). Submarine groundwater discharge in an important net source of light and middle REEs to coastal waters of the Indian River Lagoon, Florida, USA. *Geochimica et Cosmochimica Acta*, *75*(3), 825–843. https://doi.org/10.1016/j.gca.2010.11.005

Kawabe, M., Fujio, S., Yanagimoto, D., & Tanaka, K. (2009). Water masses and currents of deep circulation southwest of the Shatsky Rise in the western North Pacific. *Deep-Sea Research Part I*, *56*(10), 1675–1687. https://doi.org/10.1016/j.dsr.2009.06.003

Laukert, G., Frank, M., Bauch, D., Hathorne, E. C., Gutjahr, M., Janout, M., & Hölemann, J. (2017). Transport and transformation of riverine neodymium isotope and rare earth element signatures in high latitude estuaries: A case study from the Laptev Sea. *Earth and Planetary Science Letters*, *477*, 205–217. https://doi.org/10.1016/j.epsl.2017.08.010

Liu, Z. F., Zhao, Y. L., Colin, C., Stattegger, K., Wiesner, M. G., Huh, C. A., et al. (2016). Source-to-sink transport processes of fluvial sediments in the South China Sea. *Earth Science Reviews*, *153*, 238–273. https://doi.org/10.1016/j.earscirev.2015.08.005

Lugmair, G. W., Shimamura, T., Lewis, R. S., & Anders, E. (1983). Samarium-146 in the early solar system: Evidence from neodymium in the Allende meteorite. *Science*, *222*(4627), 1015–1018. https://doi.org/10.1126/science.222.4627.1015

Mahoney, J. B. (2005). Nd and Sr isotopic signatures of fine-grained clastic sediments: A case study of western Pacific marginal basins. *Sedimentary Geology*, *182*(1-4), 183–199. https://doi.org/10.1016/j.sedgeo.2005.07.009

Molina-Kescher, M., Frank, M., & Hathorne, E. C. (2014). Nd and Sr isotope compositions of different phases of surface sediments in the South Pacific: Extraction of seawater signatures, boundary exchange, and detrital dust provenance. *Geochemistry, Geophysics, Geosystems*, *15*, 3502–3520. https://doi.org/10.1002/2014GC005443

Pettke, T., Lee, D.-C., Halliday, A. N., & Rea, D. K. (2002). Radiogenic Hf isotopic compositions of continental eolian dust from Asia, its variability and its implications for seawater Hf. *Earth and Planetary Science Letters*, *202*(2), 453–464. https://doi.org/10.1016/S0012-821X(02)00778-1

Piepgras, D. J., & Jacobsen, S. B. (1988). The isotopic composition of neodymium in the North Pacific. *Geochimica et Cosmochimica Acta*, *52*(6), 1373–1381. https://doi.org/10.1016/0016-7037(88)90208-6

Pomiès, C., Davies, G. R., & Conan, S. M.-H. (2002). Neodymium in modern foraminifera from the Indian Ocean: Implications for the use of foraminiferal Nd isotope compositions in paleo-oceanography. *Earth and Planetary Science Letters*, *203*(3-4), 1031–1045. https://doi.org/10.1016/S0012-821X(02)00924-X

Roberts, N. L., Piotrowski, A. M., Elderfield, H., Eglinton, T. I., & Lomas, M. W. (2012). Rare earth element association with foraminifera. *Geochimica et Cosmochimica Acta*, *94*, 57–71. https://doi.org/10.1016/j.gca.2012.07.009

Seo, I., Lee, Y. I., Yoo, C. M., Kim, H. J., & Hyeong, K. (2014). Sr-Nd isotope composition and clay mineral assemblages in eolian dust from the central Philippine Sea over the last 600 kyr: Implications for the transport mechanism of Asian dust. *Journal of Geophysical Research: Atmospheres*, *119*, 11,492–11,504. https://doi.org/10.1002/2014JD022025

Serno, S., Winckler, G., Anderson, R. F., Hayes, C. T., McGee, D., Machalett, B., et al. (2014). Eolian dust input to the subarctic North Pacific. *Earth and Planetary Science Letters*, *387*, 252–263. https://doi.org/10.1016/j.epsl.2013.11.008

Shao, Y. P., Wyrwoll, K.-H., Chappell, A., Huang, J. P., Lin, Z. H., McTainsh, G. H., et al. (2011). Dust cycle: An emerging core theme in earth system science. *Aeolian Research*, *2*(4), 181–204. https://doi.org/10.1016/j.aeolia.2011.02.001

Siddall, M., Khatiwala, S., van de Flierdt, T., Jones, K., Goldstein, S., Hemming, S., & Anderson, R. (2008). Towards explaining the Nd paradox using reversible scavenging in an ocean general circulation model. *Earth and Planetary Science Letters*, *274*(3-4), 448–461. https://doi.org/10.1016/j.epsl.2008.07.044

Tachikawa, K., Arsouze, T., Bayon, G., Bory, A., Colin, C., Dutay, J.-C., et al. (2017). The large-scale evolution of neodymium isotopic composition in the global modern and Holocene Ocean revealed from seawater and archive data. *Chemical Geology*, *457*, 131–148. https://doi.org/10.1016/j.chemgeo.2017.03.018

Tachikawa, K., Athias, V., & Jeandel, C. (2003). Neodymium budget in the modern ocean and paleo-oceanographic implications. *Journal of Geophysical Research*, *108*(C8), 3254. https://doi.org/10.1029/1999JC000285

Tachikawa, K., Piotrowski, A. M., & Bayon, G. (2014). Neodymium associated with foraminiferal carbonate as a recorder of seawater isotopic signatures. *Quaternary Science Reviews*, *88*, 1–13. https://doi.org/10.1016/j.quascirev.2013.12.027

Tanaka, T., Togashi, S., Kamioka, H., Amakawa, H., Kagami, H., Hamamoto, T., et al. (2000). JNdi-1: A neodymium isotopic reference in consistency with LaJolla neodymium. *Chemical Geology*, *168*(3-4), 279–281. https://doi.org/10.1016/S0009-2541(00)00198-4

Wang, H. B., Jia, X. P., Li, K., & Li, Y. S. (2015). Horizontal wind erosion flux and potential dust emission in arid and semiarid regions of China: A major source area for East Asia dust storms. *Catena*, *133*, 373–384. https://doi.org/10.1016/j.catena.2015.06.011

Weis, D., Kieffer, B., Maerschalk, C., Barling, J., de Jong, J., Williams, G. A., et al. (2006). High-precision isotopic characterization of USGS reference materials by TIMS and MC-ICP-MS. *Geochemistry, Geophysics, Geosystems*, *7*, Q08006. https://doi.org/10.1029/2006GC001283

Wu, Q., Colin, C., Liu, Z. F., Bassinot, F., Dubois-Dauphin, Q., Douville, E., et al. (2017). Foraminiferal ε_{Nd} in the deep north-western subtropical Pacific Ocean: Tracing changes in weathering input over the last 30,000 years. *Chemical Geology*, *470*, 55–66. https://doi.org/10.1016/j.chemgeo.2017.08.022

Wu, Q., Colin, C., Liu, Z. F., Douville, E., Dubois-Dauphin, Q., & Frank, N. (2015). New insights into hydrological exchange between the South China Sea and the western Pacific Ocean based on the Nd isotopic composition of seawater. *Deep-Sea Research Part II*, *122*, 25–40. https://doi.org/10.1016/j.dsr2.2015.11.005

Xu, Z. K., Li, T. G., Clift, P. D., Lim, D. I., Wan, S. M., Chen, H. J., et al. (2015). Quantitative estimates of Asian dust input to the western Philippine Sea in the mid-late Quaternary and its potential significance for paleoenvironment. *Geochemistry, Geophysics, Geosystems*, *16*, 3182–3196. https://doi.org/10.1002/2015GC005929

Yu, Z. J., Colin, C., Laure, M., Eric, D., Arnaud, D., Gilles, R., et al. (2017). Seasonal variations in dissolved neodymium isotope composition in the Bay of Bengal. *Earth and Planetary Science Letters*, *479*, 310–321. https://doi.org/10.1016/j.epsl.2017.09.022

Yu, Z. J., Wan, S. M., Colin, C., Yan, H., Bonneau, L., Liu, Z. F., et al. (2016). Co-evolution of monsoonal precipitation in East Asia and the tropical Pacific ENSO system since 2.36 Ma: New insights from high-resolution clay mineral records in the West Philippine Sea. *Earth and Planetary Science Letters*, *446*, 45–55. https://doi.org/10.1016/j.epsl.2016.04.022

Zektser, I. S. (1996). Groundwater discharge into the seas and oceans: State of art. In R. W. Buddemeier (Ed.), *Groundwater discharge in the coastal zone, LOICZ reports & studies #8* (pp. 122–123). Texel, Netherlands: LOICZ.

Zhao, W. C., Sun, Y. B., Balsam, W., Lu, H. Y., Chen, J., & Ji, J. F. (2014). Hf-Nd isotopic variability in mineral dust from Chinese and Mongolian deserts: Implications for sources and dispersal. *Scientific Reports*, *4*(1), 5837. https://doi.org/10.1038/srep05837